IEEE Access
Multidisciplinary | Rapid Review | Open Access Journal

Received February 14, 2022, accepted March 1, 2022, date of publication March 10, 2022, date of current version March 18, 2022.

*Digital Object Identifier 10.1109/ACCESS.2022.3158372*

# A Comparative Assessment of Hybrid Parallel, Series, and Full-Electric Propulsion Systems for Aircraft Application

**ENRICO FORNARO[1], MASSIMO CARDONE[2], AND ADOLFO DANNIER[3]**
[1]Department of Industrial Engineering, University of Naples Federico II, 80125 Naples, Italy
[2]Department of Chemical, Material, and Production Engineering, University of Naples Federico II, 80125 Naples, Italy
[3]Department of Electrical Engineering, and Information Technologies, University of Naples Federico II, 80125 Naples, Italy

Corresponding author: Enrico Fornaro (enrico.fornaro@unina.it)

This research has been realized during the DIPROVEL project for the development of Technology Demonstrator of an Aeronautical Hybrid Propulsion System for Light Aircraft Applications funded by the Italian Ministry of Economic Development (MISE).

**ABSTRACT** This article presents a preliminary suitable sizing methodology for the design process of the powertrain architecture for a hybrid-electric propulsion system for ultra-light and general aviation aircraft. The main objective of this activity is to design and realize a prototype of a hybrid-electric propulsion system for Cessna 337 aircraft with a maximum take-off power of 134 kW. At the same mission, two operating strategies have been chosen, max recharge and max efficiency. The first one consists of the engine running at wide-open throttle to quickly charge the battery, while the second runs at minimum specific consumption to reduce consumption. The primary energy assessment has been conducted in all proposed propulsion configurations with the same aircraft, mission, and maximum take-off weight. The results also indicated that parallel hybrid propulsion shows a better compromise in terms of 10% energy saving, 4% $CO_2$ reduction, and mission duration.

**INDEX TERMS** Hybrid-electric aircraft, parallel, series, full-electric, training mission, energy saving, $CO_2$ reduction, Li-ion battery.

## I. INTRODUCTION

In the Flightpath 2050 report are discussed the European vision for civil aviation are defined pollution and noise limits to be achieved by 2050, goals to be reached are to reduce CO2 emission by 75%, NOx emission by 90%, and noise reduction by 65% through 2050 [1]. These values are compared to the year 2000 baseline technologies. In Fixed Wing Project N+3, similar goals have been proposed by NASA. The most important goals are highlighted: reduction of noise equal to 71dB, 70% of fuel-saving and, 75% of NOx reduction [2]. Although general aviation aircraft far outnumber civil aviation aircraft, they have not been included in the above programs, mainly due to the fact that civil aviation has a greater fuel consumption impact of about 92% in US aviation sector [3]. General aviation will follow the trend set for civil aviation, with less stringent limits, but still leading to overall improvements. In [4] have been outlined the principal field of research in airframe design, propulsion design and propulsion airframe integration. Propulsion electrification is one way to reduce gas emission, and at the same time allows to increase designs freedom and performances improvement of future aircraft. Indeed, the electrical motors provide more potential if compared to internal combustion engines, both due to their direct reduction in emissions and their inherently high power-to-weight ratio. However, their power supply highlights their great limitation for aeronautical application due to the high specific weight of the batteries. Hybrid propulsion systems can be the winner in the short to medium term because on the one hand it combines the advantages offered by fuel systems and the electric motor [5], then on the other one, it minimizes the disadvantages when taken individually. Therefore, the use of hybrid powertrains can achieve high conversion efficiencies as well as low emissions and noise pollution. Ye Xie *et al.* have discussed the state of art of aircraft powered by hybrid electric propulsion system. The paper demonstrated that the study of mid-scale hybrid airplanes can contribute the most to both researchers and practices. The small-scale hybrid such as unmanned aerial vehicles has been widely studied and put into practice, while large hybrid aircraft will be staying at the stage of concept analysis unless electrical storage technologies experiment

The associate editor coordinating the review of this manuscript and approving it for publication was Jie Tang.

evolutionary improvements [6]. Glassock *et al.* have examined a full electric and a hybrid electric propulsion for a skydiver lift. It has been shown how a short duration high power mission such as skydiving can use HEP equipped aircraft to reduce fuel consumption, CO2 emission. The skydiving mission good match the actual electrical propulsion limit, it is approximately two person-hour of flight time. Moreover, a simply configured distributed propulsion benefits the efficiency to offset the problematic aspects by the increase of HEP system weight [7]. Same consideration in terms of mission duration has been carried out in this study, where flight segments are repeated several times useful for pilots training. Usually, preliminary sizing does not require detailed knowledge of geometry, therefore is particularly suitable for determining the influence of a new propulsion architecture. Moreover, also Pornet *et al.* proposed an extension of the conventional size and performance methodology, for fuel-energy aircraft. The hybrid retrofit concept is capable of medium range mission utilizing the conventional propulsion system only based on fuel. When flying short range mission, significant fuel burn savings can be obtained by using the electrical energy of the battery. The benchmark against a conventional reference aircraft, shows in Pornet *et al.* study, a reduction of potential fuel burn up to 16% and 18% using a mix of fuel energy to electrical energy [8]. About integrated sizing of the hybrid propulsion and aircraft have been proposed by de Vries *et al.* [9] and Riboldi [10]. The first author proposed a suitable generic sizing method, applied to a regional transport aircraft, for the first stages of the design process of hybrid electric aircraft, taking into account the powertrain architecture and associated propulsion-airframe integration effects. This method is applied a hybrid electric propulsion concept featuring leading-edge distributed propulsion. The results of these studies confirm that, for the assumed technology levels and mission requirements, utilization of hybrid electric distributed propulsion does not lead any benefit at aircraft level when compared to a conventional powertrain. Therefore, de Vries *et al.* reaffirm that an integrated optimization study that considers the mission and power control profiles is necessary. These aspects have a significant influence on the resulting aircraft characteristics [9]. Riboldi presents in his work a procedure to effectively tackle the sizing problem for hybrid electric aircraft, based on an optimal approach where take-off weight is minimized, and constraints are included to assure meeting the mission performance requirements while not exceeding any technological limit. The author proposed a methodology based on hybrid-electric aircraft design that corresponds to the requirements that can be met with an all-electric solution. In this way, the weight advantages that could be obtained by implementing a hybrid-electric solution are more evident [10]. Therefore, an effective way to evaluate the performance of a hybrid powertrain is to take a high-level approach, as was investigated by Tyler S. Dean on the Tecnam P2006T aircraft [11]. In this work has been studied the propulsion system of the Cessna 337, in wich three new propulsion options have been proposed: parallel hybrid (PH), series hybrid (SH), and fully electric (FE). All proposed solutions have been carried out with the same training mission, and same maximum take-off weight (MTOW) equal to 1.700 kg. The energy consumption and $CO_2$ gas emission for each configuration have been compared with benchmark performances of the Continental IO 360. The PH propulsion configurations have been evaluated in terms of different EM size, different transmission gear ratio (GR), and different battery dimension. To carry out all investigation of the HEPS propulsion configuration has been developed a useful analysis performance model in Matlab/Simulink environment. This model has been designed to compare the main performance parameters between different solutions (e.g., parallel, series, fully electric) and it's able to be quickly reconfigurable for an assigned mission profile. This model has been developed to take in consideration engine performance maps, sometimes easily available from the manufacturers' datasheets. Therefore, it can be easily reconfigured, and it is fast in processing, so it can be efficiently used for investigating all of propulsion configurations during preliminary design. Moreover, this model has been tested and validated with experimental data in Cardone *et al.* studies [12], [13].

## II. MATERIALS AND METHODS

In Fig.1 have been shown all configurations considered, also including benchmark powertrain, called conventional. The simplified representation includes energy sources as fuel and battery, thermal motor and electric motor/generator, transmission, gear ratio (GR), and the power parts that connect these elements. Nevertheless, the effect of converters (i.e., inverters and rectifiers) can be accounted for by including their efficiency losses in the associated EM elements. All set-up configurations have been summarized in Table 1.

### A. HYBRID ELECTRIC PROPULSION ARCHITECTURE

The hybridization factor is an important index, very now known in the literature, that allows classifying hybrid propulsion. It's defined as follows:

$$HF = \frac{P_{EM}}{P_{EM} + P_{ICE}} \tag{1}$$

where $P_{EM}$ is electric motor power, and $P_{ICE}$ is internal combustion engine power. In this study, the target power has been fixed at 134 kW, where the maximum $P_{ICE}$ is 95 kW in all configurations.

#### 1) PARALLEL HYBRID–PH

The parallel hybrid has been divided into three different types. Each of these, presents a different gear ratio and weight, showed in Table 1. It should be considered that the CMD 22 engine is clutched to the propeller not directly, like the Continental, but with a gear ratio GR = 0.5. The total transmission ratio between crankshaft ICE to the propeller shaft has been maintained equal to GR = 0.5.

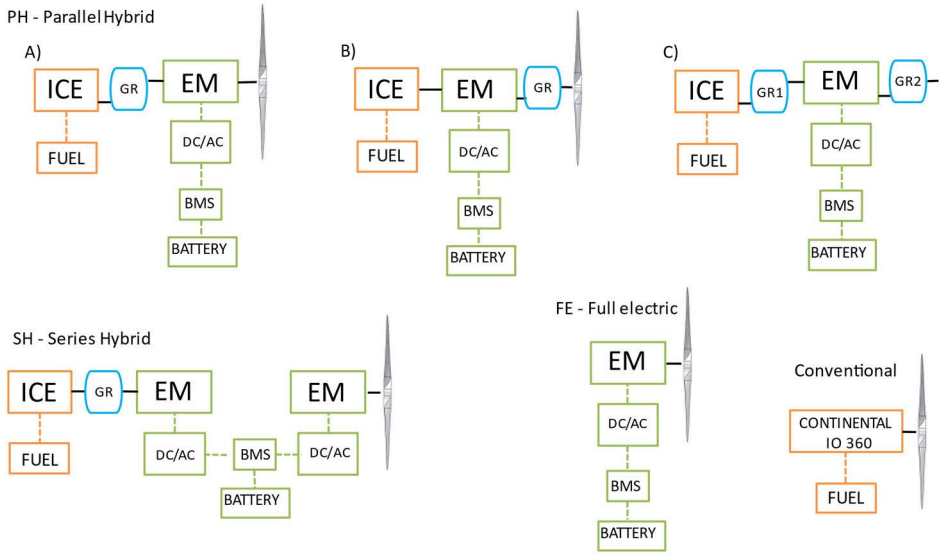


**FIGURE 1.** Scheme of all propulsion system considered: Parallel hybrid (A, B, C), series hybrid, conventional and full-electric.

The following (2) considered to define the gear ratio value.

$$GR = \frac{rpm\_Driven}{rpm\_Driver} \tag{2}$$

PH – A) The propeller has been directly coupled with the electric motor/generator. This last is coupled at CMD 22 engine through gear ratio, Fig.1 (A).

PH – B) The propeller has been coupled with electric motor/generator through gear ratio, while this last is directly coupled with CMD 22 engine, Fig.1 (B).

PH – C) The propeller has been coupled with electric motor/generator through gear ratio GR2, while this last is coupled at CMD 22 engine through another gear ratio GR1, Fig.1 (C).

This hybrid electric architecture has been proposed using two different EM sizes EMRAX 228 and 268. The hybridization factor is HF=0.29 because 39 kW of electrical power is needed to reach the target propulsion power. The gears weight has been estimated at 10 kg in all PH (A) and (B) cases, while for PH (C) with two gears double weight has been considered.

#### 2) SERIES HYBRID–SH

In this case Fig.1 (SH), the CMD 22 engine is disconnected from the propeller. For this configuration, two EM were needed. In particular, one generator connected to CMD 22 engine, and one motor connected to the propeller, both EMRAX 348. The hybridization factor in this configuration is HF=0.58, where 134kW of electric power is needed. The gear weight has been estimated at 10 kg in SH configuration, where only one gear ratio is present.

#### 3) FULLY ELECTRIC–FE

For this purpose, has been used only one electric motor EMRAX 348 Fig.1 (FE). In this configuration the hybridization factor HF=1. No gear ratio weight gain has been considered for FE configuration.

### B. MISSION PROFILE

The mission consists of a training mission where flight segments are repeated several times for pilot training. In particular, the flight profile has been shaped in a sequence of repeated climbs, cruises, base lags, descents, landing, but only one take-off. This mission is also called ''touch-and-go'', in Table 2 all mission segments have been defined. The mission repetitions are strictly dependent on battery size and onboard fuel quantity. The model input parameters consist of each mission sequence of time $t$, aircraft velocity $v$, and propeller speed $rpm$.

**TABLE 1.** Hybrid electric propulsion configuration.

| Configuration | Motor | Gear Ratio | HF | GR weight [kg] |
|---|---|---|---|---|
| Conventional | CONTINENTAL IO 360 | - | 0 | - |
| Parallel Hybrid | CMD22 EMRAX 228 | A) GR=0.5<br>B) GR=0.5<br>C) GR1=0.875, GR2=0.571 | 0.29 | A) 10<br>B) 10<br>C) 20 |
| Parallel Hybrid | CMD22 EMRAX 268 | A) GR=0.5<br>B) GR=0.5<br>C) GR1=0.725, GR2=0.689 | 0.29 | A) 10<br>B) 10<br>C) 20 |
| Series Hybrid | CMD22 EMRAX 348 | GR=0.5 | 0.58 | 10 |
| Fully Electric | EMRAX 348 | - | 1 | - |

### C. AIRCRAFT AND PROPELLER

The Cessna 337 is a twin-engine utility aircraft built in a push-pull configuration. Its engines have been mounted in the nose and rear of its fuselage. This aircraft handles differently from a conventional twin-engine aircraft in that if one engine

**TABLE 2. Training mission profile.**

| Mission sequence | Time [s] | Aircraft Velocity [km/h] | Altitude [m] | Power [kW] | Propeller Speed [rpm] |
|---|---|---|---|---|---|
| Start-up and taxi | 10 | 10 | 0 | 50 | 1735 |
| Take-off | 20 | 130 | 0 - 91 | 134 | 2530 |
| Climb | 300 | 160 | 91 - 762 | 134 | 2590 |
| Cruise | 300 | 224 | 762 | 134 | 2798 |
| Descent | 240 | 194 | 762 - 244 | 45 | 2123 |
| Hold | 60 | 194 | 244 | 40 | 2080 |
| Descent | 30 | 160 | 244 - 152 | 35 | 1860 |
| Approach | 15 | 160 | 152 - 304 | 30 | 1807 |
| Landing | 10 | 130 | 304 - 0 | 20 | 1531 |

fails, the plane does not yaw toward that engine. Moreover, the minimum controllable flight speed is guaranteed, but the performances in terms of speed and, particularly, rate of climb are affected. The main reasons that led to choosing this aircraft in this study are:

- possibility to flight using only one engine. For this reason, has been chosen to install the hybrid-electric propulsion system in the rear of the fuselage. While in the front position to leave Continental IO 360 engine. This configuration provides more safety during the development phases. In fact, upon engine failure on take-off, the pilot would have the choice of stopping or continuing the take-off without unbalanced thrust as a conventional twin-engine airplane;

- high useful load to board bulky and heavy battery. The manufacturer declares that using 134 kW the Maximum Take-off Weight (MTOW) is 1700 kg, with a useful load about to 705 kg [14]. In Table 3 are summarized principal characteristics and performances of Cessna 337.

**TABLE 3. Characteristics and performance of the Cessna 337 aircraft.**

| Characteristics | Type/Value |
|---|---|
| Front Engine | Continental IO360 |
| Rear Engine | HEPS |
| Front propeller diameter | 1930 mm |
| Rear propeller diameter | 1720 mm |
| Velocity never exceed (VNE) | 361 km/h |
| Stall Speed Flaps Up | 128 km/h |
| Stall Speed Flaps Down | 112 km/h |
| Maximum Take-off weight | 1700 kg |
| Empty weight | 995 kg |
| Useful load | 705 kg |

In addition, a new propeller has been chosen to match hybrid-electric propulsion to the Cessna 337. This investigation has been considered a fixed pitch of 22°, with 1720 mm of diameter, two blades, and inertia $I_{PROP} = 0.35$ kg $\times$ m$^2$. Moreover, for each hybrid-electric propulsion configuration, the same propeller has been used, this means that will be transferred the same power of the propulsion at specific aircraft velocity v and propeller speed rpm. In Fig.2 each marker point is representative of the training mission phase defined in Table 2. Through (3.a), (3.b), (3.c), and (3.d) obtained by application of Momentum Theory and McCormick coefficient curves of power $C_P$, torque $C_q$ and thrust $C_T$ [15], [16], the propeller performance curve at different aircraft velocity v can be obtained in all rpm regime as shown in Fig.2.

$$J = v/nD \tag{3.a}$$

$$P = C_P \rho n^3 D^5 \tag{3.b}$$

$$M = C_q \rho n^2 D^5 \tag{3.c}$$

$$T = C_T \rho n^2 D^4 \tag{3.d}$$

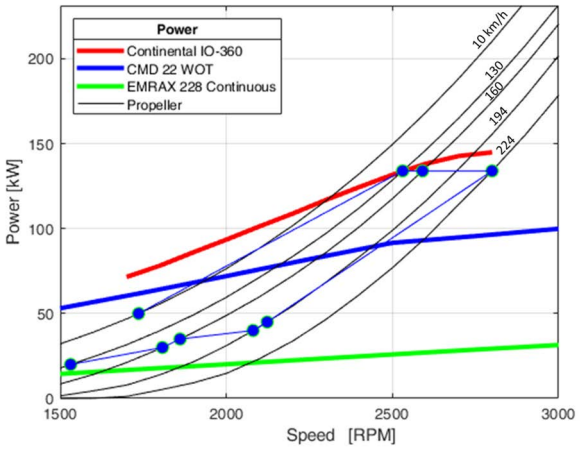


**FIGURE 2. Engines and Propeller power curves, at different aircraft speed v. Marker points representative of mission phase.**

### D. INTERNAL COMBUSTION ENGINE

The conventional engine equipped on Cessna 337 is the Continental IO 360 is a 156 kW (210 hp) maximum engine power, fuel-injected, air-cooled, horizontally opposed six-cylinder, direct-drive aircraft engine, manufactured by Continental Motors (Continental Aerospace Technologies, Inc., 2039 S. Broad Street, Mobile, Alabama 36615, USA).

The CMD 22 is a 95 kW (127 HP) maximum engine power, fuel-injected, air-cooled, horizontally opposed four-cylinder, geared aircraft engine GR = 0.5, manufactured by CMD Engine (CMD Spa., 2 Via Pacinotti, San Nicola la Strada 81020, Caserta, Italy). In Table 4 are summarized principal performance and technical specifications of both engines'. The engine's weight indicated in Table 4 refers to the wet conditions ready to flight. In Fig.3 shows the Continental IO 360 and CMD 22 performance torque and specific consumption curves. For the CMD 22 has been calculated ideal operating line. This curve represents the minimum engine specific consumption in all function regimes; it has been used during maximum efficiency run cases.

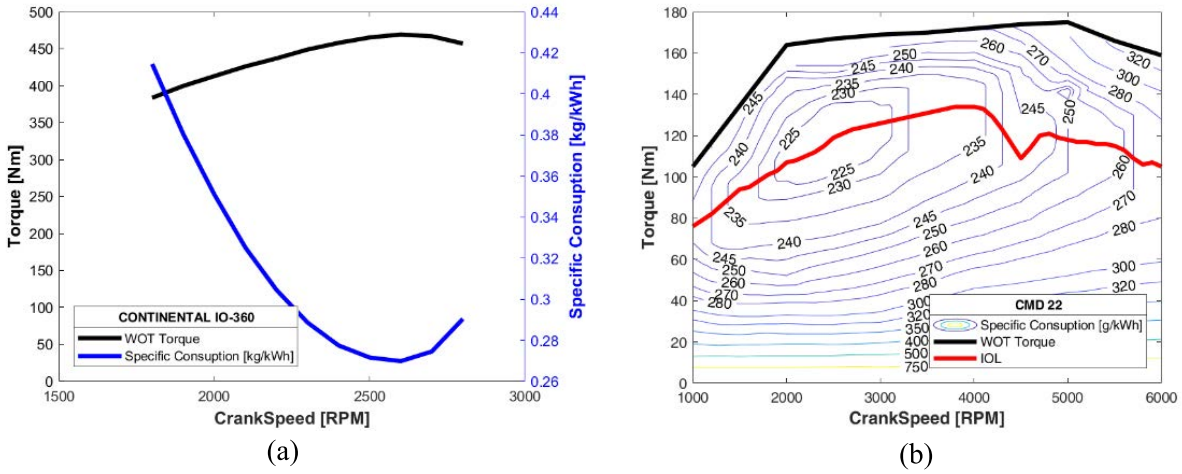


**FIGURE 3.** (a) Continental IO-360 torque and specific consumption curves; (b) CMD 22 specific consumption map. Wide open throttle (WOT) torque (black curve), and ideal operating line (IOL) torque (red curve).

**TABLE 4.** Engine performance and technical specifications.

| Technical specification | | CONTINENTAL IO 360 | CMD 22 |
|---|---|---|---|
| Bore | [mm] | 112.776 | 100 |
| Stroke | [mm] | 98.552 | 70 |
| 1 Cyl. Disp. | [cm3] | 984.4 | 549.5 |
| Displacement tot | [cm3] | 5906.6 | 2198 |
| Compression ratio | [-] | 8.5:1 | 1.1:1 |
| Cylinder N° | [-] | 6 | 4 |
| Firing order | [-] | 1-6-3-2-5-4 | 1-3-2-4 |
| Prop. drive ratio | [-] | 1:1 | 1:2 |
| Prop. driven rotation | [-] | Clockwise | Clockwise |
| Weight (wet) | [kg] | 190 | 90 |
| Weight/Power | [kg/kW] | 1.014 | 0.895 |

### E. ELECTRIC MOTOR/GENERATOR AND COOLING SYSTEM

To address the challenges of electrification in aircraft, electric machines are affected by a constant search for innovation. The aim is to obtain electric machines with high power density and torque. In order to achieve this goal a new design approach can be adopted: starting from the mathematical model of the electric machine a suitable relation between the requested torque and the required volume is needed [17]. The most promising machines that bring the main requirements of an electric traction motor in terms of high power density, high torque density, high speed range, high efficiency, high reliability and low costs is definitely represented by motors Permanent Magnet Synchronous Machine (PMSM). In this preliminary study have been chosen EMRAX electrical motors/generators. In particular, it is a PMSM axial flux motors/generators with a high number of pole pairs whose operating speeds is compatible with the considered application, which guarantees at the same time high values of torque density. Three types of EMRAX Low Voltage (LV) electric motors have been considered, shown in Table 5. Only EMRAX 268 performance curves have been shown in Fig.4. The manufacturer has three different possible voltage levels for each model, so as to ensure greater flexibility for the different types of use. In this specific case, the model best suited to the constraints of our hybrid system is represented by the low voltage configuration. Indeed, the dc-link voltage is linked to the choice of energy storage and therefore to the amount of energy required in the different phases of the mission. The lowered values of energy required suggest a configuration of the battery pack with a reduced number of cells in series which, therefore, requires the choice of a low voltage configuration of the electric machine.

**TABLE 5.** Electric motor performance.

| Performance | | 228 CC LV | 268 CC LV | 348 CC LV |
|---|---|---|---|---|
| Continuous motor power at load RPM | [kW] | 62 | 107 | 210 |
| Maximal rotation speed | [RPM] | 5500 | 4500 | 4000 |
| Continuous motor torque | [Nm] | 120 | 250 | 500 |
| Continuous motor current | [Arms] | 450 | 500 | 550 |
| Specific load speed (max load) | [RPM/1V dc] | 34 | 18 | 9.5 |
| Max battery voltage | [Vdc] | 160 | 250 | 420 |
| Motor efficiency | [%] | 92 - 98 | 92 - 98 | 92 - 98 |
| Technical specification | | | | |
| Weight | [kg] | 12.3 | 20.3 | 41.5 |
| Diameter | [mm] | 228 | 268 | 348 |
| Width | [mm] | 86 | 91 | 107 |
| IEM = Electric motor inertia | [kgm$^2$] | 0.0355 | 0.0664 | 0.3654 |

Obviously, based on this choice in order to obtain high performance, it is necessary to use a combined cooling system, where air and water have been used, so as to ensure the correct disposal of the different rates of energy losses mainly attributable to Joule losses. The total cooling system weight including pump, exchanger, and storage tank has been estimated equal to 15 kg in all configurations. Only in Series Hybrid, where 1 electric motor ed 1 generator have been considered, the total cooling system weight has been estimated equal to 30 kg.

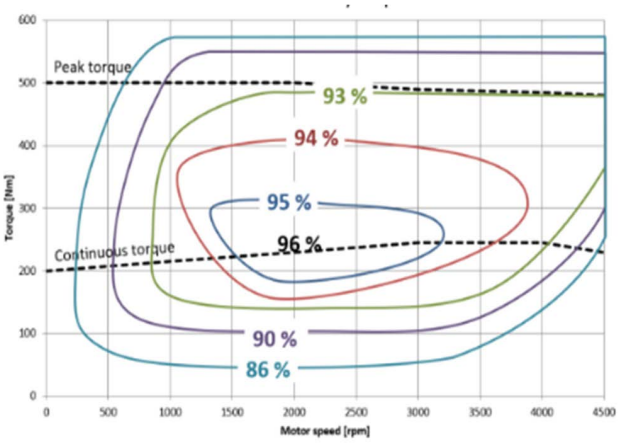


**FIGURE 4.** Electric motor performance curves representative of the EMRAX 268.

### F. ENERGY STORAGE SYSTEM

The sizing of the Energy Storage System (ESS) must satisfy different constraints both of an electrical and mechanical nature. In particular, with reference to the electrical aspects, the ESS must guarantee: a sufficient energy for the different phases of the mission, DC-link voltage values compatible with the chosen motor-generator, in order to favor an effective control through the inverter, and C-rate values able to make the necessary power available during the supply phase or to receive the recovery power during the regeneration phase. Each of the aforementioned aspects participates in defining the configuration of the ESS, making it possible to identify even the minimum technical specifications that the single-cell battery must present. There are different configurations possible for each fixed cell. The optimal solutions, given the nature of the application, are those where the energy density stands out. Some authors size the battery on the nominal capacity needed to guarantee a defined mission profile, imposing a maximum discharge coefficient [18]. In this study, Li-Ion rechargeable batteries have been considered thanks to their good performance in terms of energy density. On the other hand, concerning mechanical constraints, the maximum battery weight has been chosen so that all useful load is exploited. In addition to the engines and transmission weight, other loads, three passengers, 25 kg of baggage, a cooling system, and battery management systems were considered for all configurations. To evaluate the optimal configuration of the ESS for the considered application, once the previous constraints were defined, the single Li-Ion cell was modeled through a battery dynamic model to predict the ESS performance. In Table 6 the most important parameters taken into account have been shown [19]–[21].

### G. PROPULSION SYSTEM MODELLING

The proposed model Fig.5 has been designed to compare the performance between different propulsion configurations (e.g., parallel, series, fully electric) and it's able to be quickly reconfigurable. The model control parameter is the propeller speed, this is dependent on the mission profile in Table 2. The propeller speed error $rpm_{error}$ has been obtained by (4), where the difference between input $rpm_{mission}$ and calculated $rpm_{calulate}$, also normalized respect to mission profile.

$$rpm_{error} = \frac{rpm_{mission} - rpm_{calulate}}{rpm_{mission}} \tag{4}$$

Through $rpm_{error}$ in input at two PID controllers, one for ICE and one for EM has been possible to regulate throttle position, and so also torque available at the propeller. Moreover, two controller strategies have been considered in order to investigate hybrid-electric configuration for the best compromise in terms of efficiency, and emission save.

Fastly charge mode strategy consists of battery charge at max available ICE torque in all regimes, this configuration has been obtained when the engine work at wide-open throttle (WOT) Fig.3 (b - black curve). Economy charge mode consists of battery charge at minimum ICE specific consumption, this configuration has been obtained when the engine work at corresponding ideal operating line IOL Figure 3 (b - red curve). The internal combustion engine torque $M_{ICE}$ has been described through a 1-D look-up table, where torque is a function of the rotational speed. Another 2-D look-up has been used to evaluate ICE specific consumption. Similarly, also for the electric motor torque $M_{IEM}$ has been used a 1-D look-up table, and a 2-D look-up has been used to evaluate EM efficiency. The propeller torque has been modeled using (2.a), (2.c), where 2-D look-up tables have been used to insert McCormick coefficients curves [15], [16]. Equations (5.a), (5.b), and (5.c) describe, for each proposed

$$\text{Conventional} \quad M_{ICE(t)} - M_{PROP(t)} = I\frac{(\omega_{(t+1)} - \omega_{(t)})}{\Delta t} \tag{5.a}$$

$$\text{Parallel Hybrid} \quad M_{ICE(t)} \pm M_{EM(t)} - M_{PROP(t)} = I\frac{(\omega_{(t+1)} - \omega_{(t)})}{\Delta t} \tag{5.b}$$

$$\text{Series Hybrid and Full Electric} \quad M_{EM(t)} - M_{PROP(t)} = I\frac{(\omega_{(t+1)} - \omega_{(t)})}{\Delta t} \tag{5.c}$$

configuration, the dynamic coupling model between ICE, EM, and propeller evaluated at the propeller shaft. Where $M_{ICE(t)}$ is the ICE torque, $M_{EM(t)}$ is the EM torque motor (if positive) or generator (if negative), $M_{PROP(t)}$ is the propeller's resistant torque, $I$ is the system's overall moment of inertia consists of $I_{EM}$, $I_{PROP}$ and $I_{RESIDUAL}$ sum (last term

**TABLE 6.** Li-Ion battery parameters.

| Parameters | | Li-Ion |
|---|---|---|
| E0 = battery constant voltage | [V] | 3.366 |
| Q = battery capacity | [Ah] | 3.4 |
| R = internal resistance | [Ω] | 0.01 |
| K = polarization constant | [V/Ah] | 0.0076 |
| A = exponential zone amplitude | [V] | 0.26422 |
| B = exponential zone time constant inverse | [$Ah^{-1}$] | 26.5487 |
| e = energy density | [Wh/kg] | ~200 |

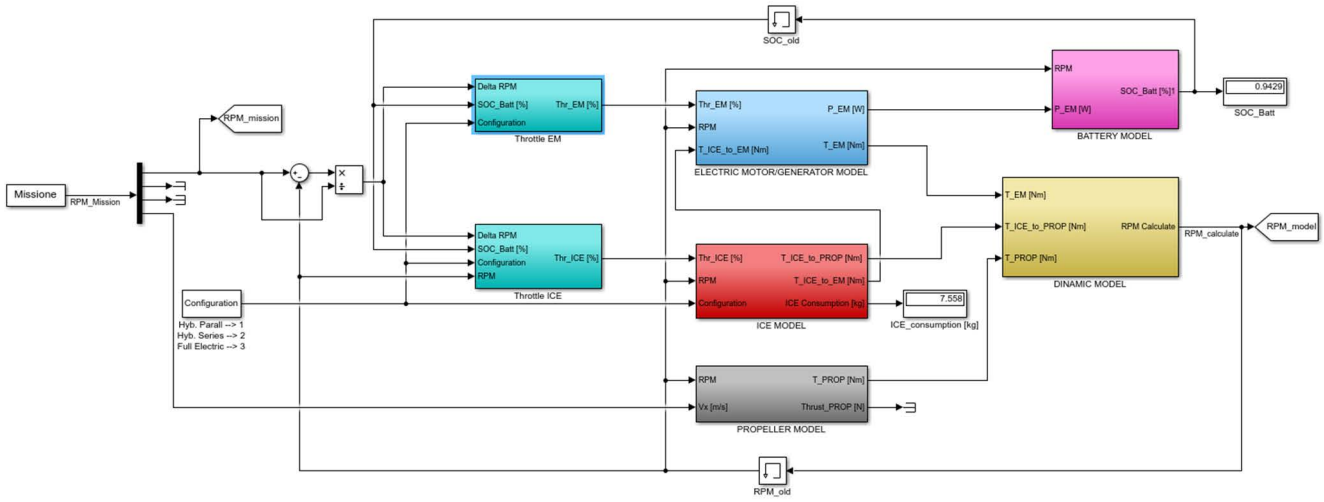


**FIGURE 5.** Block scheme of the MATLAB Simulink overall model.

include estimation of ICE, gear ratios inertia), and $\omega$ is the propeller speed in rad/s, $\Delta t$ is the model increase time step.

The Li-Ion battery has been modelled through an equivalent electric circuit [19]. Follow are showed the mathematical relationships (6) and (7) used to describe the battery.

$$V_{batt} = E_0 - R \cdot i - K\frac{Q}{Q - it}\left(it + i^*\right) + A \cdot exp(-B \cdot it) \tag{6}$$

$$V_{batt} = E_0 - R \cdot i - K\frac{Q}{it - 0.1Q}i^* - K\frac{Q}{Q - it}it + A \cdot exp(-B \cdot it) \tag{7}$$

where $i$ is the discharging or charging current, $i^*$ is the filtered current value, $Q$ is the battery capacity, and $it$ is the current time integral plus the initial battery charge. Moreover, $E_0$, $R$, $K$, $A$, and $B$ refers to the actual battery cell's characteristics or calibration constants Table 6.

### 1) MODEL SET-UP

As already mentioned, all HEPS has been carried on with the same Maximum take-off Weight equal to 1.700 kg, where useful aircraft payloads are equal to 705 kg. Table 7 has been reported all propulsion components weight for each propulsion configuration. For ICE and EM declared by the manufacturer's weight has been chosen. The cooling system weight has been estimated at 15 kg in all cases, only for SH configuration double weight has been considered because two electric motors have been considered. In addition, three crew passengers each 80 kg, and 25 kg of baggage have been considered. The battery weight has been estimated through specific energy density. The cells number of series and parallel cells have been chosen to maximize the electric storage and at the same time has been obtained equal energy stored for parallel hybrid propulsion configuration. The fuel quantity ensures the mission execution and ensures equal weight in all configurations. In Table 8 the main batteries parameters have been listed for all proposed cases. Lastly, the battery management system (BMS) and inverter weights have been estimated at 17 kg in all cases.

## III. RESULTS

The model outputs provide many parameters both for ICE and EM how power, torque, the battery state of charge SOC, voltage, current, and fuel consumption. Therefore, it is possible to compare different propulsion configurations for the same mission, so evaluate fuel consumption and $CO_2$ emission. Fig.6 refers to PH-268 (A) configuration, where Fig.6 (a) shows mission input speed, dashed line, and calculated ones by the model green line. Moreover, Fig.6 (b) are shows ICE, EM, and Propeller power. Power negative refers to a resistive load (i.e., propeller) that is always resistive while EM changes when switching the motor to generator mode.

The parallel hybrid PH – 228 (B) and PH – 268 (B) configurations must be discarded because in both cases the EM exceeds the maximum speed range. This condition can be viewed in Fig.7 (a1, a2, b1, b2) by plotting the mission points on the operating area of the EM. For the EMRAX 228, the speed exceeds is little, while for EMRAX 268 the speed limit exceeds is much.

Also, there are no problems during mission execution when the EMRAX 268 Fig.7 (b1, b2) and the EMRAX 228 Fig.7 (a1, a2) have been used in the PH - 268 (A) and PH - 228 (A) configurations, respectively. Only a slight excess of torque is required for the EMRAX 228. Therefore, it's important to provide an adequate cooling system so that the EM temperature doesn't exceed the limit. A better compromise, between A and B solution, is using motor EMRAX 228 in PH - 228 (C) configuration, where neither maximum mission speed exceeds the electric motor limits, nor maximum torque exceeds the electric motor continuous torque Fig.7 (a1, a2).

**TABLE 7.** Summary of weights in kilograms of all proposed configurations.

| Configuration | ICE | EM | BMS + Inverter | Gear & Coupling | Cooling System | Passenger | Baggage | Battery | Fuel | Tot. Useful Payload |
|---|---|---|---|---|---|---|---|---|---|---|
| Conventional | 190 | - | - | - | - | 240 | 25 | 0 | 250 | 705 |
| PH - 228 (A) | 90 | 12 | 17 | 10 | 15 | 240 | 25 | 220 | 76 | 705 |
| PH - 228 (B) | 90 | 12 | 17 | 10 | 15 | 240 | 25 | 220 | 76 | 705 |
| PH - 228 (C) | 90 | 12 | 17 | 20 | 15 | 240 | 25 | 220 | 66 | 705 |
| PH - 268 (A) | 90 | 20 | 17 | 10 | 15 | 240 | 25 | 220 | 68 | 705 |
| PH - 268 (B) | 90 | 20 | 17 | 10 | 15 | 240 | 25 | 220 | 68 | 705 |
| PH - 268 (C) | 90 | 20 | 17 | 20 | 15 | 240 | 25 | 220 | 58 | 705 |
| SH - 348 | 90 | 83 | 17 | 10 | 30 | 240 | 25 | 172 | 38 | 705 |
| FE - 348 | 0 | 41.5 | 17 | - | 15 | 240 | 25 | 367 | - | 705 |

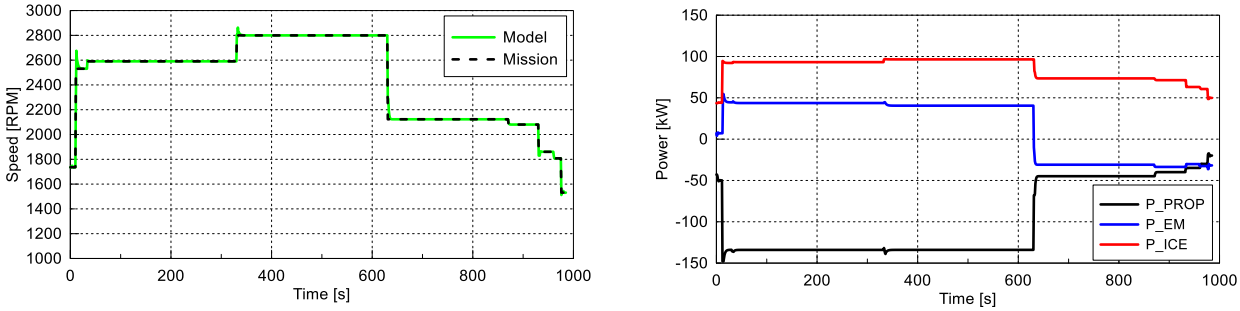


**FIGURE 6.** (a) Required speed mission in dashed line and calculated speed in green line; (b) Instantaneous ICE, EM, and Propeller power. These figures refer to the PH-268 (A) configuration.

**TABLE 8.** Battery design parameters.

| Configuration | N° cells Series | N° cells Parallel | Nominal Voltage [V] | Nominal Capacity [Ah] | Tot. Battery Energy [kWh] |
|---|---|---|---|---|---|
| Conventional | 0 | 0 | 0 | 0 | 0 |
| PH - 228 (A) | 38 | 101 | 128 | 343 | 44 |
| PH - 228 (B) | 38 | 101 | 128 | 343 | 44 |
| PH - 228 (C) | 38 | 101 | 128 | 343 | 44 |
| PH - 268 (A) | 62 | 62 | 209 | 211 | 44 |
| PH - 268 (B) | 62 | 62 | 209 | 211 | 44 |
| PH - 268 (C) | 62 | 62 | 209 | 211 | 44 |
| SH - 348 | 100 | 30 | 337 | 102 | 34 |
| FE - 348 | 100 | 64 | 337 | 217 | 73 |

Similarly, the same investigation has been conducted for the EMRAX 268 motor in the PH - 268 (C) configuration in Fig.7 (b1, b2).

In addition, no problems are found with the operation of the EMRAX 348 motor Fig.7 (c1, c2) when used for the Series and all-electric configurations. The above considerations do not change if the electric motor works in motor mode whether fast charge strategy or the economy charge will be chosen but, change the working points only during charge mode when electric motor works as a generator. Fig.8 and Fig.9 have been shown the difference between PH-228 (A) and SH-348 configurations. The first figure shows the operating mission points referred to the fast charge (a1, b1) and economy charge mode (a2, b2) on CMD 22 specific consumption map, while in the second figure same configuration is plotted to highlight the power shape during the mission. Fig.8 (a1, a2) shows that the functional engine points move from max torque in wide-open throttle condition to the minimum specific consumption around the ideal operating line. Fig.9 (a1, a2) are shown both strategies, where the power required for the propeller is the same in both cases. After a time of 630s, during landing maneuvers, the ICE follows different paths depending on the adopted recharge strategy. The same considerations are true for series hybrid configuration shown in Fig.8 (b1, b2) and Fig.9 (b1, b2). In Fig.8 (b1), using the fast charge strategy, the ICE runs at WOT and 5500rpm of crankshaft speed until the end, while in Fig.8 (b2) adopting the economy charge strategy, the ICE running at 5500rpm but follow the minimum consumption curve IOL.

Fig.9 (b1, b2) clearly shows that the ICE starts to run after some time, when the state of battery charge is less than 0.9. The ICE power doesn't transfer to the propeller but is used for battery charge. For SH-348 configuration the SOC and fuel consumption could be seen in Fig.10 (a1, a2), while current and voltage required at the battery in Figure 10 (b1, b2). in this case the battery SOC follows three different trends, first one is from SOC 1 to 0.9, where only EM is running this trend is equal for both strategies. From SOC 0.9, until the end of the cruise at the time of 630s, where adopting fast charge strategy a lower SOC slope is visible if compared to economy charge. In fact, during fast charge strategy less energy, and so less current is required to the battery, how can see in

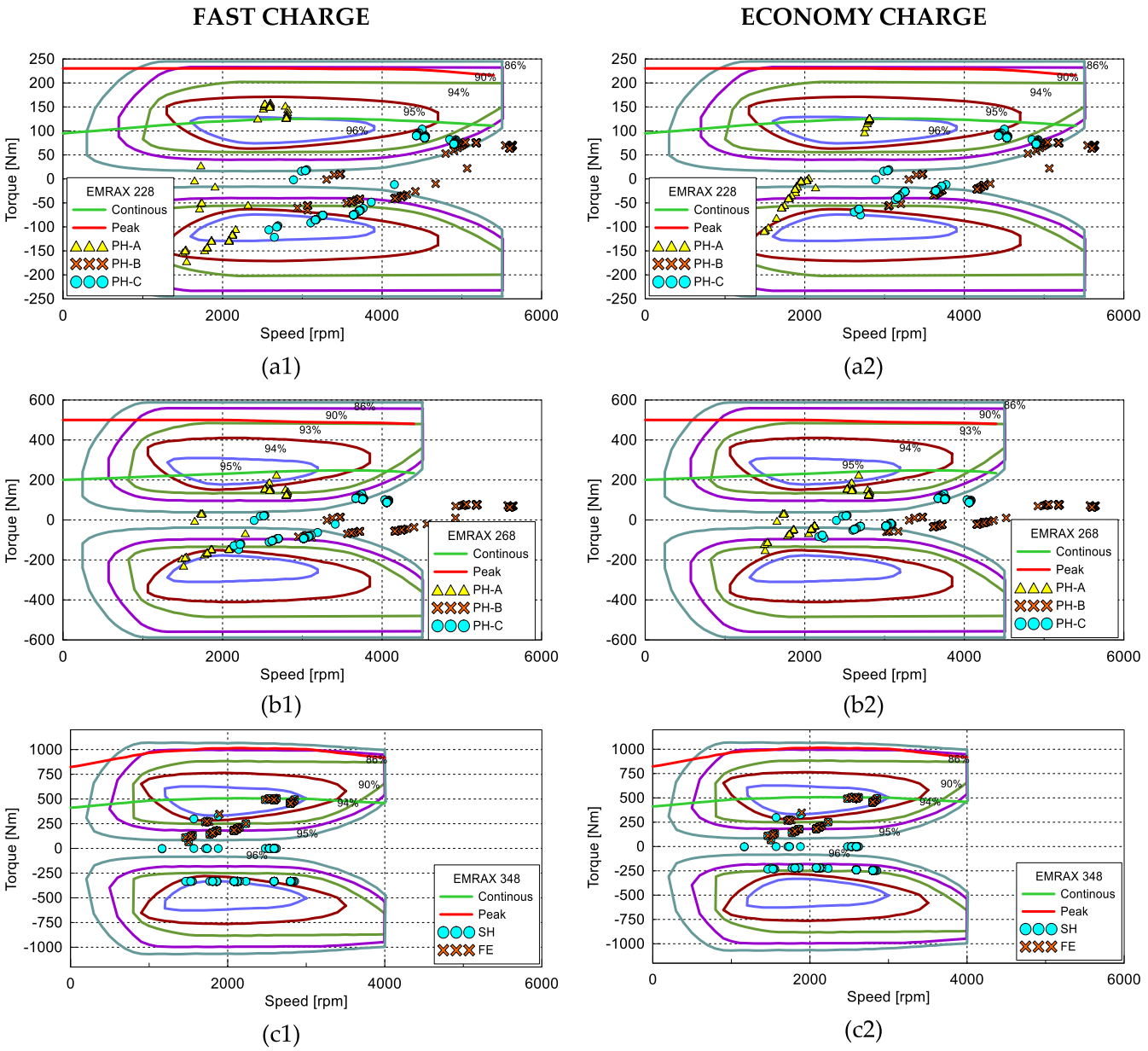


**FIGURE 7. Operating mission points referred to the electric motor (a1, a2) using EMRAX 228, (b1, b2) using EMRAX 268, (c1, c2) using EMRAX 348 were (1) refer to fast charge and (2) economy charge.**

Fig.10 (b1, b2). The last trend during landing maneuvers, a major power is available in fast charge if compared to economy charge strategy. Also, at these stages, when more current is available to charge the battery, the higher the fuel consumption will be. The battery current plotted in Fig.10 (b1, b2) doesn't total energy available at the electrical motor, but only net make available from the battery side. In other words, it represents the difference between the required current by an electric motor and supplied by a generator.

### A. ENERGY CONSUMPTION

In all configurations, the total energy consumption $E_{total}$ has been calculated as sum of the fuel and battery energy contribution through (8)

$$E_{total} = E_{fuel} + E_{batt} \tag{8}$$

where, energy $E_{fuel}$ depends on the fuel consumption, while $E_{batt}$ depends on the battery energy consumption, both calculated through equation (9) and (10)

$$E_{fuel} = M_{fuel} \cdot H_i \tag{9}$$

$$E_{batt} = \frac{(SOC_i - SOC_f) \cdot E_{capacity} \cdot 3600}{\eta_{el}} \tag{10}$$

where, $M_{fuel}$ is the mass of fuel consumption, $H_i$ is the AvGas 100 specific net heat of combustion $H_i \cong 43.5$ MJ/kg [22],

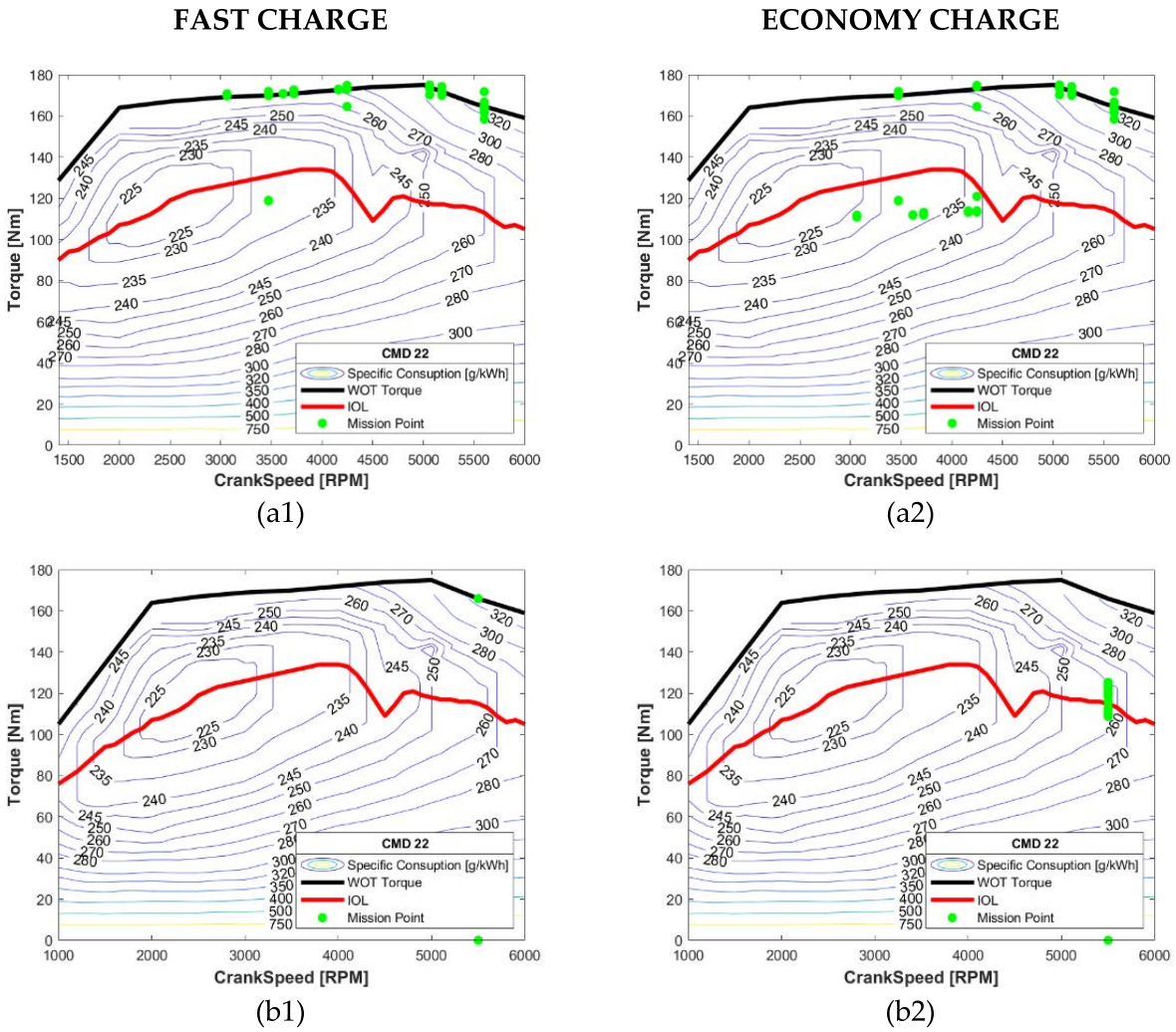


**FIGURE 8.** Operating mission points referred to the CMD 22 specific consumption map in PH-228 (A) (a1, a2), SH-348 (b1, b2), where (1) refer to fast charge and (2) economy charge.

$SOC_i$ and $SOC_f$ refers respectively to initial and final battery state of charge, $E_{capacity}$ is total battery energy capacity (see Table 8), $\eta_{el}$=0.554 (at 2018) National Electricity Grid efficiency referred to Italian State [23].

It has been assumed that the electricity stored in the battery has been taken from the National Electricity Grid and that this is fully charged at the start of the mission $SOC_i$=1.

The percentage of primary energy has been obtained by total energy comparison between conventional $E_{total\_convenzional}$ and $E_{total\_HEPS}$ configurations through the following (11)

$$\Delta E_{\%} = \frac{E_{total\_convenzional} - E_{total\_HEPS}}{E_{total\_convenzional}} \cdot 100 \qquad (11)$$

Table 9 are shown the results in terms of energy comparisons in all propulsion cases, excluding parallel hybrid in B cases, for both strategies fast charge and economy charge. In Fig.11 are highlighted maximum number of mission repetition. These values have been calculated knowing final $SOC_f$,

**TABLE 9.** Summary of energy consumption.

| Configuration | FAST CHATGE | | | ECONOMY CHARGE | | |
|---|---|---|---|---|---|---|
| | $M_{fuel}$ [kg] | $SOC_f$ [-] | $\Delta E_{\%}$ | $M_{fuel}$ [kg] | $SOC_f$ [-] | $\Delta E_{\%}$ |
| Conventional | 8.30 | - | | 8.30 | - | |
| PH - 228 (A) | 7.16 | 0.92 | 7.35 | 6.63 | 0.88 | 10.95 |
| PH - 228 (C) | 7.16 | 0.91 | 7.00 | 6.61 | 0.88 | 10.71 |
| PH - 268 (A) | 7.29 | 0.92 | 6.05 | 6.61 | 0.88 | 10.90 |
| PH - 268 (C) | 7.18 | 0.90 | 5.81 | 6.61 | 0.86 | 9.54 |
| SH - 348 | 7.66 | 0.83 | -2.53 | 4.12 | 0.66 | 29.52 |
| FE - 348 | - | 0.67 | 56.13 | - | 0.67 | 56.13 |

through following (12) round to the nearest integer.

$$N^{\circ} = \frac{1}{1 - SOC_f} \qquad (12)$$

As highlighted in Table 9 the most advantageous HEPS configuration is fully electric, with 56.13% energy saving. The final $SOC_f$ permit only three mission repetitions with this architecture. Similarly, mission repetition for series hybrid

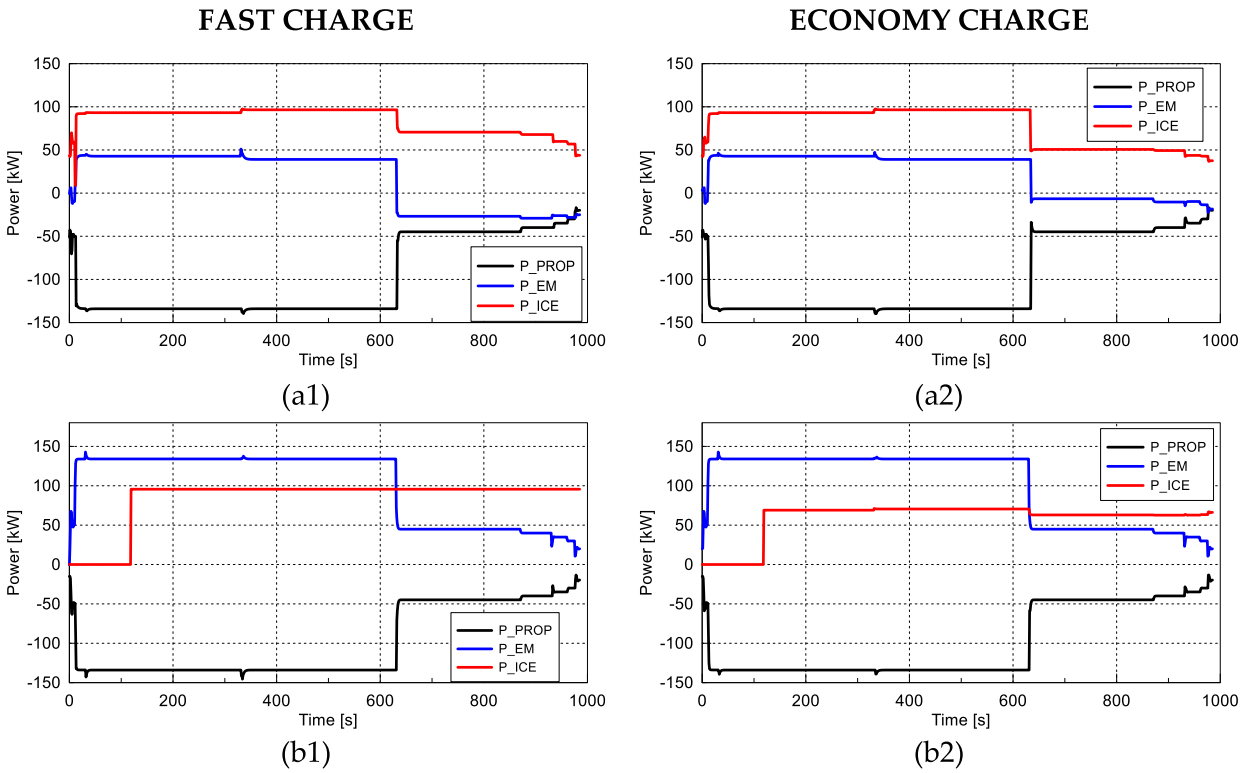


**FIGURE 9.** Mission power profile for PH-228 (A) (a1, a2) and SH-348 (b1, b2) configurations, where (1) refer to fast charge and (2) economy charge.

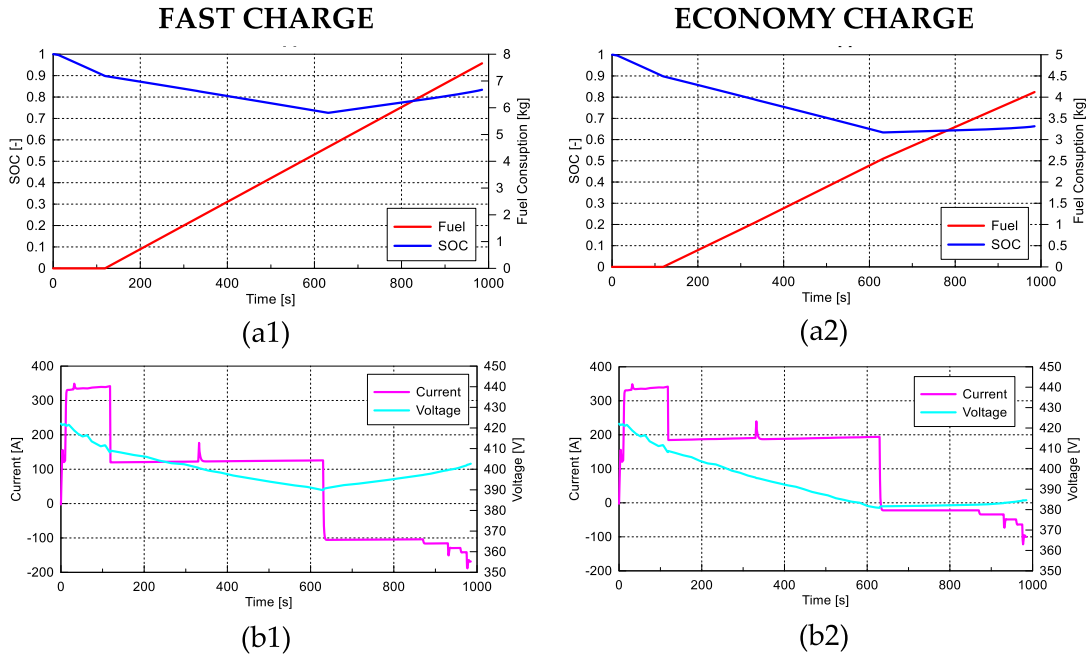


**FIGURE 10.** Mission profile in SH-348 configuration (a1, a2) SOC and fuel consumption, and (b1, b2) battery current, and voltage.

but less energy saving has been obtained 29.52% when economy charge strategy is used. Parallel hybrid configurations showed a good compromise in terms of energy-saving around 10% using economy charge, until a maximum of 8 repetitions of mission, while around 7% energy saving in fast charge with 12 maximum repetitions. The difference between

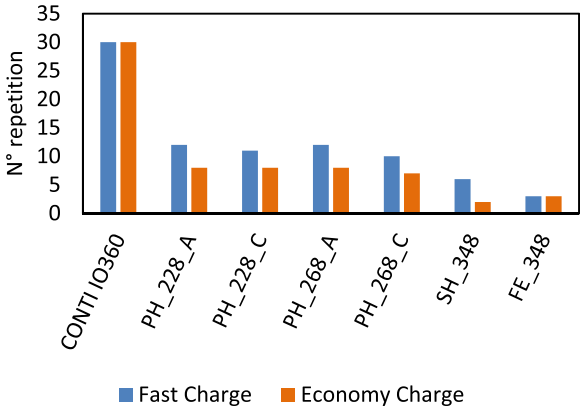


**FIGURE 11.** Maximum number of mission training repetition.

primary energy-saving in (A) and (C) cases has been highlighted in Table 9. Them finds justification in the better functional configuration of (A) respect (C) where the operative points of the EM motors are included in the highest efficiency zone, how clearly shown in Fig.7 (a1, a2, b1, b2).

### *B. $CO_2$ EMISSION*

The mass of $CO_2$ gas emission $M_{total\_CO_2}$ has been estimated in all cases by the sum of directly $CO_2$ emission by fuel consumption $M_{fuel\_CO_2}$ and indirect emission linked to grid energy consumption necessary to charge the battery $M_{batt\_CO_2}$.

$$M_{total\_CO_2} = M_{fuel\_CO_2} + M_{batt\_CO_2} \tag{13}$$

$$M_{fuel\_CO_2} = M_{fuel} \cdot 3.16 \tag{14}$$

$$M_{batt\_CO_2} = E_{batt} \cdot 444.4 \tag{15}$$

where, $M_{fuel}$ is the mass of fuel consumption, assuming the average chemical formula of AvGas 100 to be $C_8H_{15}$, the approximated amount of Carbon Dioxide emitted in the atmosphere for each kilograms of fuel is $3.16 kg_{CO_2}/kg_{fuel}$ [5], $E_{batt}$ depends of the battery energy consumption (see equation 9), $444.4 kg_{CO_2}/kWh$ (at 2018) National Electricity Grid efficiency referred to Italian State [23]. The percentage of $CO_2$ gas mass emission has been obtained by comparison between conventional $M_{total\_CO_2\_convenzional}$ and $M_{total\_CO_2\_HEPS}$ configurations through the following (16).

$$\Delta CO_{2\%} = \frac{M_{total\_CO_2\_convenzional} - M_{total\_CO_2\_HEPS}}{M_{total\_CO_2\_convenzional}} \cdot 100 \tag{16}$$

Table 10 and Fig.12 are shown the results in terms of $CO_2$ gas mass emission comparisons in all propulsion cases, excluding parallel hybrid in B cases, for both strategies fast charge and economy charge.

The proposed procedure can be made by exploiting different types of mission profiles as described in [24].

**TABLE 10.** Summary of $CO_2$ gas emission.

| Configuration | FAST CHATGE | | | ECONOMY CHARGE | | |
|---|---|---|---|---|---|---|
| | $M_{fuel\_CO_2}$ [kg] | $M_{batt\_CO_2}$ [kg] | $\Delta CO_{2_{\%}}$ | $M_{fuel\_CO_2}$ [kg] | $M_{batt\_CO_2}$ [kg] | $\Delta CO_{2_{\%}}$ |
| Conventional | 26.31 | - | - | 26.31 | - | - |
| PH - 228 (A) | 22.70 | 2.85 | 2.92 | 21.03 | 4.07 | 4.61 |
| PH - 228 (C) | 22.70 | 3.01 | 2.28 | 20.97 | 4.28 | 4.05 |
| PH - 268 (A) | 22.76 | 2.73 | 3.10 | 20.97 | 4.19 | 4.38 |
| PH - 268 (C) | 22.76 | 3.43 | 0.46 | 20.97 | 4.80 | 2.06 |
| SH - 348 | 24.28 | 4.57 | -9.65 | 13.06 | 9.28 | 15.07 |
| FE - 348 | - | 19.3 | 26.6 | - | 19.3 | 26.6 |

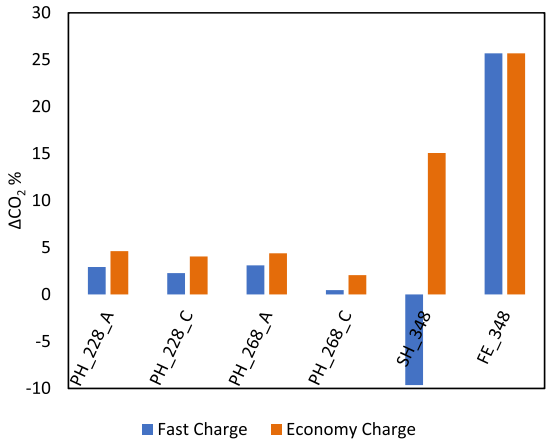


**FIGURE 12.** Summary of the percentage variation of the $CO_2$ gas emission.

## IV. CONCLUSION

The results obtained using parallel hybrid propulsion show in PH – 228 (B) and PH – 268 (B) configurations that directly couple the electric motor to the internal combustion engine must be discarded because both the EM exceeds the maximum speed range. The energy saving and reduction of $CO_2$ gas emission are obtained in all configurations except for series hybrid when fast charge strategy is used because the ICE specific consumption and EM efficiency don't guarantee a real benefit. The most advantageous energy 56% and $CO_2$ reduction 26.6% solution is the fully electric configuration, but the final $SOC_f$, allow the pilot only two mission repetitions. The series hybrid configuration, only using economy charge strategy, can reduce energy 29.5% and $CO_2$ by 15% but only two mission repetitions are possible. Therefore, the parallel hybrid propulsion could be the best compromise in terms of energy, and $CO_2$ saving, and mission duration. In the PH - 228 (C) and PH - 268 (C) configurations, two gear ratios have been used, the EM is enabled to work in a possible functional range, but the operating points don't fit into best efficiency. Therefore, the benefits are limited if compared to (A) configurations.

In conclusion, the PH - 228 (A) and PH - 268 (A) are the best compromises configurations. An average 10% of the benefit in terms of energy-saving and 4% of CO2 gas reduction using if the economy charge strategy are used.

For the PH - 228 (A) configuration is important to supervise the maximum temperature because overcoming continuous torque is needed for some mission phases. Moreover,

is mandatory for both electrical engines to evaluate the EM shaft robustness that must be able to transfer the sum of ICE and EM torque to the propeller. Moreover, the adoption of a different strategy can increase the advantages by around 30% but against decries the mission duration in terms of the number of repetitions. During this preliminary study, good results have been obtained in terms of energy-saving and $CO_2$ gas emission reduction, if compared with benchmark performances using Continental IO 360.

According also to [11] the better compromise in terms of energy saving, $CO_2$ reduction and mission duration could be identified in the parallel hybrid configuration. Future studies will be needed on strategies optimization, that take into account engines efficiency and mission target, how example mission duration or $CO_2$ reduction.

## REFERENCES

[1] *Flightpath 2050: Europe's Vision for Aviation: Maintaining Global Leadership and Serving Society's Needs*, European Union, Maastricht, The Netherlands, 2011, doi: doi/10.2777/50266.
[2] K. Suder, "Overview of the NASA environmentally responsible aviation Project's propulsion technology portfolio," in *Proc. 48th AIAA/ASME/SAE/ASEE Joint Propuls. Conf. Exhib.*, Jul. 2012, p. 4038, doi: 10.2514/6.2012-4038.
[3] Federal Aviation Administration. *FAA Aerospace Forecast Fiscal Years 2021-2041*. Accessed: 2020. [Online]. Available: https://www.faa.gov/data_research/aviation/aerospace_forecasts/
[4] S. W. Ashcraft, A. S. Padron, K. A. Pascioni, G. W. Stout, Jr., and D. L. Huff, "Review of propulsion technologies for N+3 subsonic vehicle concepts," NASA, Glenn Res. Center, Cleveland, OH, USA, Tech. Rep. NASA/TM-2011-217239, 2011.
[5] C. Friedrich and P. A. Robertson, "Hybrid-electric propulsion for automotive and aviation applications," *CEAS Aeronaut. J.*, vol. 6, no. 2, pp. 279–290, Jun. 2015, doi: 10.1007/s13272-014-0144-x.
[6] Y. Xie, A. Savvarisal, A. Tsourdos, D. Zhang, and J. Gu, "Review of hybrid electric powered aircraft, its conceptual design and energy management methodologies," *Chin. J. Aeronaut.*, vol. 34, no. 4, pp. 432–450, Apr. 2021, doi: 10.1016/j.cja.2020.07.017.
[7] R. Glassock, M. Galea, W. Williams, and T. Glesk, "Hybrid electric aircraft propulsion case study for skydiving mission," *Aerosp.*, vol. 4, no. 3, 2017, Art. no. 3, doi: 10.3390/aerospace4030045.
[8] C. Pornet, C. Gologan, P. C. Vratny, A. Seitz, O. Schmitz, A. T. Isikveren, and M. Hornung, "Methodology for sizing and performance assessment of hybrid energy aircraft," *J. Aircr.*, vol. 52, no. 1, pp. 341–352, Jan. 2015, doi: 10.2514/1.C032716.
[9] R. de Vries, M. Brown, and R. Vos, "Preliminary sizing method for hybrid-electric distributed-propulsion aircraft," *J. Aircr.*, vol. 56, pp. 1–17, Oct. 2019, doi: 10.2514/1.C035388.
[10] C. E. D. Riboldi, "An optimal approach to the preliminary design of small hybrid-electric aircraft," *Aerosp. Sci. Technol.*, vol. 81, pp. 14–31, Oct. 2018, doi: 10.1016/j.ast.2018.07.042.
[11] T. S. Dean, G. E. Wroblewski, and P. J. Ansell, "Mission analysis and component-level sensitivity study of hybrid-electric general-aviation propulsion systems," *J. Aircr.*, vol. 55, no. 6, pp. 2454–2465, Nov. 2018, doi: 10.2514/1.C034635.
[12] M. Cardone, B. Gargiulo, and E. Fornaro, "Modelling and experimental validation of a hybrid electric propulsion system for light aircraft and unmanned aerial vehicles," *Energies*, vol. 14, no. 13, p. 3969, 2021, doi: 10.3390/en14133969.
[13] M. Cardone, B. Gargiulo, and E. Fornaro, "Development of a flexible test bench for a hybrid electric propulsion system," in *Proc. IEEE Int. Workshop Metrol. Automot.*, Oct. 2021, pp. 221–225, doi: 10.1109/MetroAutomotive50197.2021.9502723.
[14] *Super Skymaster 337—Owners's Manual*, Cessna Aircraft Company, Wichita, KA, USA, 1971. [Online]. Available: https://cessna.txtav.com/en
[15] P. M. Sforza, "Propellers," in *Theory of Aerospace Propulsion*, P. M. Sforza, Ed. Oxford, U.K.: Butterworth-Heinemann, 2017, pp. 487–524, doi: 10.1016/B978-0-12-809326-9.00010-5.
[16] B. W. McCormick, *Aerodynamics, Aeronautics, and Flight Mechanics*. Hoboken, NJ, USA: Wiley, 1994. [Online]. Available: https://books.google.it/books?id=ALRkQgAACAAJ
[17] A. Dannier, E. Fedele, and M. Coppola, "Sizing approach of high torque density motors for aircraft application," in *Proc. Int. Symp. Power Electron., Electr. Drives, Autom. Motion (SPEEDAM)*, 2020, pp. 497–501, doi: 10.1109/SPEEDAM48782.2020.9161871.
[18] T. Donateo and L. Spedicato, "Fuel economy of hybrid electric flight," *Appl. Energy*, vol. 206, pp. 723–738, Nov. 2017, doi: 10.1016/j.apenergy.2017.08.229.
[19] O. Tremblay and L.-A. Dessaint, "Experimental validation of a battery dynamic model for EV applications," *World Electr. Veh. J.*, vol. 3, no. 2, pp. 289–298, Jun. 2009, doi: 10.3390/wevj3020289.
[20] T. Chen, Y. Jin, H. Lv, A. Yang, M. Liu, B. Chen, Y. Xie, and Q. Chen, "Applications of lithium-ion batteries in grid-scale energy storage systems," *Trans. Tianjin Univ.*, vol. 26, no. 3, pp. 208–217, Jun. 2020, doi: 10.1007/s12209-020-00236-w.
[21] A. Dannier, L. Ferraro, R. Miceli, L. Piegari, and R. Rizzo, "Numerical and experimental validation of a $LiFePO_4$ battery model at steady state and transient operations," in *Proc. 8th Int. Conf. Exhib. Ecol. Veh. Renew. Energies (EVER)*, 2013, pp. 1–6, doi: 10.1109/EVER.2013.6521570.
[22] (May 2020). *ExxonMobil Aviation Gasolines*. [Online]. Available: https://www.exxonmobil.com/en-us/commercial-fuel/pds/gl-xx-avgas-series
[23] ISPRA. (2010). *Fattori di Emissione Atmosferica di Gas a Effetto Serra Nel Settore Elettrico Nazionale e Nei Principali Paesi Europei*. [Online]. Available: https://www.isprambiente.gov.it
[24] T. Donateo and R. Totaro, "Hybridization of training aircraft with real world flight profiles," *Aircr. Eng. Aerosp. Technol.*, vol. 91, no. 2, pp. 353–365, Feb. 2019, doi: 10.1108/AEAT-01-2018-0036.

**ENRICO FORNARO** graduated in mechanical engineering at the University of Naples Federico II, in 2014. He received the master's (second level) degree in management engineering for public safety. He is currently pursuing the Ph.D. degree with the University of Naples Federico II, where he is working on aeronautical hybrid systems. Until 2018, he worked with the Research and Development Department of CMD Engine company, contributing to aeronautical certification process of the CMD22 engine. Since 2018, he has been employed as a State Police Officer at the Italian Ministry of Interior.

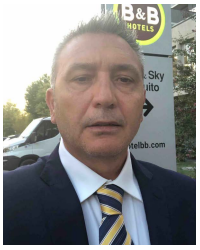

**MASSIMO CARDONE** received the M.S. degree in mechanical engineering from the Università degli Studi di Napoli Federico II, in 1997, and the Ph.D. degree in fluid machinery from the Università degli Studi di L'Aquila, in 2001.

He is currently an Associate Professor in fluid machinery and energy systems with the Department of Chemical Engineering, Materials and Industrial Production (DiCMAPI), Università degli Studi di Napoli Federico II. His research interests include internal combustion engine (performance and exhaust emission) also fueled with non-conventional fuels, experimental-analytical study on turbocharger and green mobility (e-bike), and hybrid propulsion systems.

**ADOLFO DANNIER** graduated in electrical engineering at the University Federico II of Naples, in 2003, where he received the Ph.D. degree in electrical engineering in 2008, with a dissertation on multilevel converters with fault-tolerant structures. Since 2020, he has been an Associate Professor with the University Federico II in "Converters, electrical machines, and drives" and teaches "Modelling of electric machines and converters" and "Power electronic converter." Active in the research topics of his scientific sector, he collaborated with the national and international research projects, as attested by numerous and significant scientific publications. The research interests include high-performance dynamic drives with PM motors, conversion equipment, and electrical energy storage for electric vehicles and for the integration of renewable energy sources.